

Upper Mantle Structure in the Alpine Zone from Surface Wave Tomography*

Yu. G. Farafonova^a, Foreign Member of the RAS G. F. Panza^{b,c},
T. B. Yanovskaya^a, and C. Doglioni^d

Received March 27, 2007

DOI: 10.1134/S1028334X0707029X

The present-day Alpine region began to form more than 100 Ma ago with the subduction of a Tethyan branch beneath the Adriatic plate, eventually arriving at

the collisional stage of the European continental lithosphere at about 40 Ma ago. Presently, Africa is moving northward relative to Europe at a rate of about

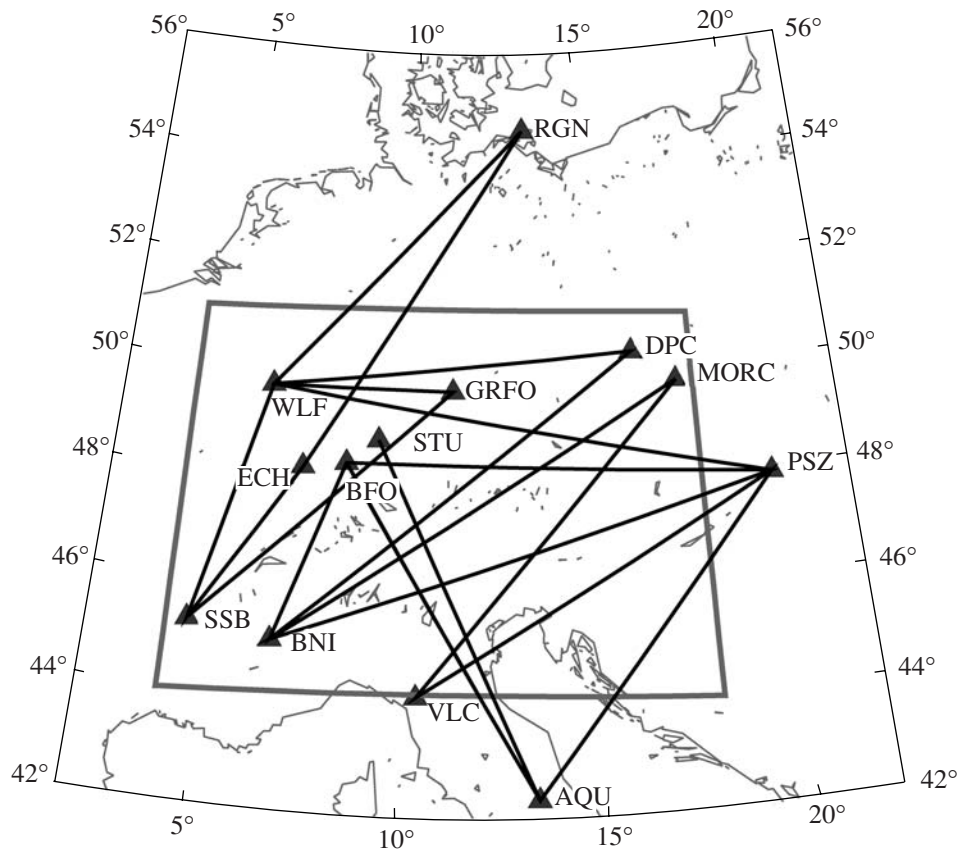


Fig. 1. Locations of stations and station-to-station paths.

* This article was translated by the authors.

^aSt. Petersburg State University, NIIF SPbGU, Ul'yanovskaya 1, Petrodvorets, St. Petersburg, 198504 Russia

^bDipartimento di Scienze della Terra, Università degli studi di Trieste, Via Weiss 4, 34127 Trieste, Italy

^cThe Abdus Salam International Centre for Theoretical Physics (ICTP), Strada Costiera 11, 34100 Trieste, Italy

^dDipartimento di Scienze della Terra, Università La Sapienza, P. le A. Moro 5, Box 11, 00185, Roma, Italy

0.5 cm/yr, but most of the shortening is absorbed in the Southern Tyrrhenian Sea. The eastern Alps overlap with the Dinarides subduction, where the Adriatic plate is rather subducting underneath Eurasia. For a better understanding of the geodynamic processes in the Alpine–Dinaric region, a reliable knowledge of the lithosphere–asthenosphere system structure is needed. However, existing information on the upper mantle structure obtained from body and surface wave tomography data [1–4] is fragmentary and sometimes contradictory.

This paper presents the results of the reconstruction of the velocity structure in the Alpine upper mantle from new data on the phase velocities of Love and Rayleigh waves. Phase velocities have been determined with the two-station method [5] from the records at pairs of stations located in Central Europe (Fig. 1) over a period range from 15 to 125 s.

For each path between the stations, dispersion curve is determined by averaging the velocity measurements from ten earthquakes. We use teleseismic records of the earthquakes with epicenters at opposite azimuths and located at the same great circle arc with the stations with a tolerance of 0.3° (difference of azimuths to the two selected stations). In such a way, it has been possible to improve the precision as compared with earlier measurements [1, 5]. The average standard error of the averaged velocities turns out to be 0.06 km/s and never exceeds 0.1 km/s.

The standard scheme of surface wave tomography—2D tomography of surface wave velocities corresponding to fixed periods followed by the inversion of local dispersion curves into vertical 1D velocity sections—could not be reliably applied due to the limited number of available paths. Therefore, we used a reversed scheme: inversion of the dispersion curves for each of the two-station paths into S-wave velocity profiles versus depth followed by 2D tomography of these S-wave velocities profiles at selected fixed depths.

The crust has been approximated with flat layers of fixed constant velocities. The investigation of the influence of such and other a priori choices on the final S-wave velocity models of the uppermost 250 km of the lithosphere–asthenosphere system is outside the purposes of the present paper and will be the subject of a forthcoming investigation, but will not alter the general picture we present here. The velocity variation in the upper mantle has been assumed to be a piece-wise linear function in order to eliminate jumps in velocities between different paths at the same depth that could be introduced by a homogeneous-layer approximation. To improve the stability of the results, the path averaged cross sections are determined by two inversion approaches: the Monte-Carlo method [6] and linear inversion by the conjugate gradient method. With the Monte-Carlo method, the mean velocity section has been determined jointly with its standard error that turned out to be about 0.1 km/s on average.

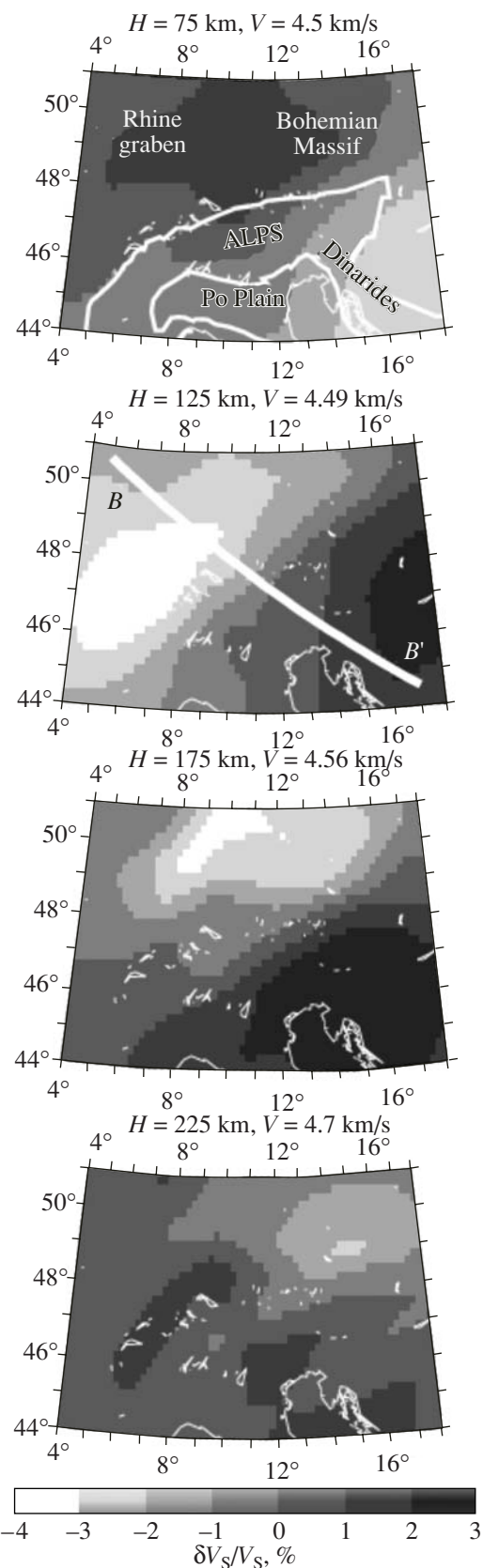


Fig. 2. Maps of horizontal variations of S-wave velocity at the depths of 75–225 km with respect to mean velocities at the corresponding depths. Mean velocity values are indicated above each map.

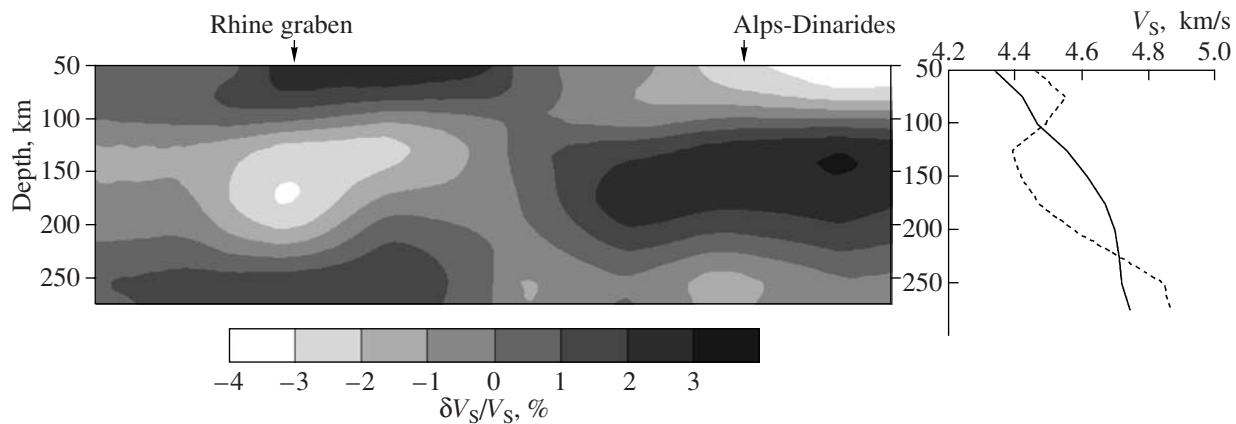


Fig. 3. Variations of S-wave velocity in the vertical section along the profile BB' shown in Fig. 2. The plot on the right side shows variations of S-wave velocity with depth in the points indicated by arrows; dashed line, under the Rhine graben; solid line, under Alps.

Velocity cross sections of SV- and SH-waves obtained by the inversion of Rayleigh and Love dispersion curves, respectively, are a little different, and this indicates the existence of some vertical anisotropy in the upper mantle. SH-wave velocity is always larger than SV-wave velocity, the anisotropy coefficient being 3–4% on average, and never exceeding 7%. Due to the limited amount of available data, we did not analyze the SH and SV velocity cross sections separately, but we preferred to determine the mean section by averaging SH- and SV-based models.

In this way, the path averaged S-wave velocity models have been determined at depths from 50 to 275 km with a step of 25 km. These data have been used for the determination of the horizontal variations of velocity at the corresponding depths by 2D tomography [7]. Figure 2 shows the velocity variations at the depths from 75 to 225 km, with respect to the reference values given in Fig. 2.

From the distribution of the two-station paths (Fig. 1), we can conclude that the best resolution can be obtained in the direction crossing the majority of paths, i.e., in the SE–NW direction. Therefore, a 2D vertical velocity cross section (% variation in Fig. 3) has been constructed along a profile in this direction (BB' in Fig. 2). In Fig. 3, variations of absolute velocity with depth in two points on the profile marked by arrows are shown on the right.

From Fig. 3, a distinct difference is seen between the structures under Alps–Dinarides and the Molasse basin merging into the Rhine graben already evidenced by [8]. A sharp boundary coinciding in the horizontal plane with the northern boundary of the Alpine zone is observed between these two domains (Fig. 2): it separates the upper mantle under the Alps (thick lithosphere and absence of asthenosphere) from that under the European slab (low velocity in the 70–200 km depth range). At the same time, the European slab is characterized by high velocities in the mantle lid.

Local high velocity bodies under the Alps have been found not only from surface wave dispersion analysis [1, 3] but also from P-wave travel time residuals by tomography methods [2, 4, 9]. In [9], the P-wave model obtained after smoothing shows an extended high-velocity zone in the depth range from 100 to 200 km, which extends along the strike of the Alpine arc (NE–SW) and dips to the SE. Our results are in agreement with [9] as far as the existence of a high-velocity zone under the Alps is concerned, but as [1, 3] they cast some doubts on the dipping of this zone to the SE. The regional high-velocity anomaly beneath the alpine orogen merges into the high-velocity anomaly of the Dinarides subduction zone. The central and eastern Alps are rather confirmed to be a doubly vergent Alpine collisional belt related to the classical model in which the European and Adriatic lithospheres are the lower and the upper plate of the Alpine subduction zone, respectively [10, 11]. This is opposite to the recent conflicting interpretation in which the Adriatic plate is considered to subduct beneath Europe [9]. The Adriatic plate is subducting NE-ward beneath the Eurasia plate only along the Dinarides, which are an independent subduction zone, although interfering with the eastern Alps at their northwestern termination.

ACKNOWLEDGMENTS

This work was supported by the Russian Foundation for Basic Research (project no. 05-05-64164), the INTAS (grant no. 04-83-381), and the ALPS-GPSQUAKENET Project funded by the EU Program Interreg III-B “Alpine Space.”

REFERENCES

1. S. Mueller, and G. F. Panza, in *The Origin of Arcs*, Ed. by F.C. Wezel (Elsevier, Amsterdam, 1986), pp. 93–113.
2. V. Babuska, J. Plomerova, and M. Granet, *Tectonophysics* **176**, 137 (1990).

3. Z. J. Du, A. Michelini, and G. F. Panza, *Phys. Earth Planet. Int.* **106**, 31 (1998).
4. C. Piromallo and A. Morelli, *J. Geophys. Res.* **108** (B2), 2065 (2003).
5. G. F. Panza, *Pageoph* **114**, 753 (1976).
6. A. Tarantola, *Inverse Problem Theory* (Elsevier, Amsterdam, 1987).
7. P. G. Ditmar and T. B. Yanovskaya, *Izv. Akad. Nauk SSSR, Fiz. Zemli* **6**, 30 (1987).
8. G. F. Panza, in *Second EGT-Workshop: The Southern Segment*, Ed. by S. Mueller and D.A. Galson (European Science Foundation, Venice, 1985), pp. 47–51.
9. E. Kissling, S.M. Schmid, R. Lippitsch, and J. Ansorge, in *European Lithosphere Dynamics* (Geol. Soc. London, 2006), Vol. 32, pp. 129–145.
10. G. F. Panza and S. Mueller, *Mem. Soc. Geol. Ital.* **33**, 43 (1978).
11. J. Kummerow, R. Kind, P. Oncken, et al., *Earth Planet. Sci. Lett.* **225**, 115 (2004).